XLI CILAMCE
XLI Ibero-Latin American Congress on Computational Methods in Engineering
16-19 November, 2020 FOZ DO IGUAÇU PARANÁ - BRAZIL

Application of double Helmholtz resonators in an ICE intake manifold to increase the air mass flow rate

Wender P. de Oliveira[1], Sérgio de M. Hanriot[1], Jaqueline M. Queiroz[1]

[1]*Dept. of Mechanical Engineering, Pontifical Catholic University of Minas Gerais*
Av. Dom José Gaspar, 500, 30535-610, Belo Horizonte/MG, Brazil
wender.oliveira@sga.pucminas.com.br, *hanriot@pucminas.br* , *jaquelinequeiroz@pucminas.br*

Abstract. Wave phenomena that occur in the intake manifold can either increase or decrease the volumetric efficiency of internal combustion engines (ICEs). In this work, a numerical and experimental investigation is carried out to evaluate the influence of the intake manifold components on the intake flow rate. In order to calculate its natural frequency, analytical expressions were developed using the acoustic theory by means of the Transfer Matrix Method (TMM). The numerical results were obtained using a one-dimensional computational code based on the Characteristics Method. The experimental tests in unsteady condition were conducted using a flow test bench equipped with a four-cylinder engine in two conditions: with only two intake valves operating and with all four operating. The numerical and experimental results were compared and a good agreement between the data was observed, thus confirming the numerical code's capacity to reproduce this type of phenomenon. The insertion of the double-chamber Helmholtz resonator increased the air mass flow rate more significantly in the four-cylinders configurations, compared to the two-cylinders manifolds. The two-cylinders configurations had an increase in flow rate up to 38.6% in the speed of 1200 rpm, while the higher increase in the four-cylinders with the insertion of the resonator was only 3.4% in the speed of 1600 rpm.

Keywords: Double Helmholtz resonators, intake manifold, pulsating flow, transfer matrix method.

1 Introduction

Studies show that volumetric efficiency is mainly influenced by the pressure inside the cylinder during the short period of time that precedes the intake valve closing [1–4]. In addition to reduction on the noise level in intake and discharge systems, the Helmholtz resonator can be used to adjust the phases of the pressure pulses that reach the intake valve port, at the end of the intake phase [5].

Resonators have as their main application in the industry the acoustic attenuation. Works such as Igarashi and Toyama [6–8], Munjal [9] and Cai and Mak [10,11] have evaluated the reduction in the level of acoustic noise in the most diverse geometries and configurations of resonators. The influence of Helmholtz resonators on the volumetric efficiency of internal combustion engines (ICEs) has been studied by authors such as Bortoluzzi et al. [12], Hanriot et al. [13], Queiroz [14,15]; Hanriot, Queiroz and Maia [16], among others.

This work has as main objective the study of the pressure wave phenomena and their impacts on the mass air flow rate and consequently the change in the ICE volumetric efficiency curve. The insertion of devices such as Helmholtz resonator and plenum and the variation of their geometry and position in the intake manifold were analyzed experimentally, through flow test bench, and numerically, applying the Characteristics Method.

2 Theoretical Analysis

During the intake phase, the valve opening and the piston movement from BDC to the TDC produces a depression inside the combustion chamber compared to the pressure in the intake runner. Assuming that the runner was theoretically of infinite size, this pressure difference would cause a rarefaction pulse that would travel along

the runner and would not be reflected, since the pipe is infinite. In real systems with finite dimensions, the rarefaction pulse is reflected in the form of a compression pulse after reaching an obstacle. As the rarefaction and compression pulses continue to move during the engine operation, there is an overlap of these waves forming an instantaneous pressure wave that can be either compression, if the compression pulse is greater than the rarefaction pulse, or rarefaction, if the rarefaction pulse is greater than that of compression.

The Helmholtz resonator is a device capable of amortizing the pressure fluctuations existing in the intake manifold of internal combustion engines. It consists of a volumetric chamber connected to the main pipe of the intake system through a pipe called neck. The oscillations in the volume of air inside the resonator's neck cause the pressure of the resonator cavity to increase, so that it absorbs this energy that later returns to the system during another cycle. In addition to this energy absorption, there is a damping due to the viscous friction of the air caused by the contact of the oscillatory movement of the air volume with the resonator's neck [2].

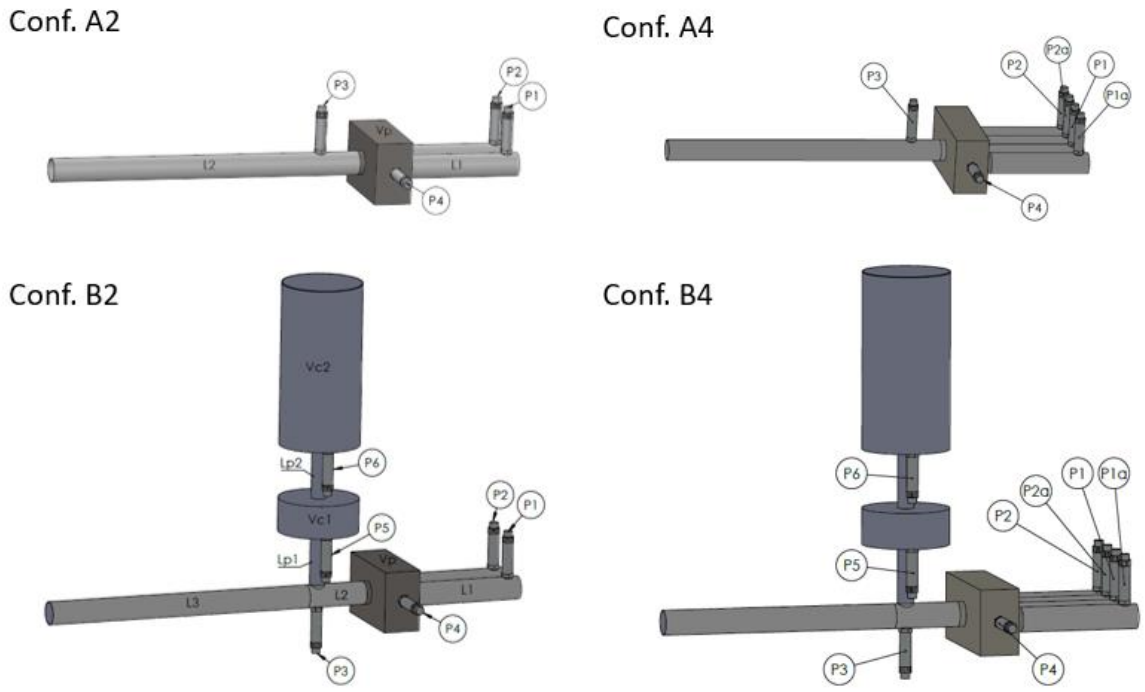

Figure 1. Intake manifold configurations

Table 1. Component's dimensions of each studied configuration

	A [cm²]	A_p /A_{p1}/A_{p2} [cm²]	L_1 [cm]	L_2 [cm]	L_3 [cm]	L_{p1} [cm]	L_{p2} [cm]	V_p [L]	V_{C1} [L]	V_{C2} [L]
Conf. A	8.04	5.07	20	280	-	-	-	1.2	-	-
Conf. B	8.04	5.07	20	7	273	10	10	1.2	1	5

Figure 1 shows the four intake manifold configurations which are analyzed in this work. Configurations A are composed by two or four runners (two in config. A2 and four in config. A4), one plenum and one secondary pipe. Configurations B are composed by two or four runners (two in config. B2 and four in config. B4), one plenum and one secondary pipe, with the addition of a double-chamber Helmholtz resonator. The measurements for all three configurations are shown in Tab. 1.

2.1 Transfer Matrix Model

The Transfer Matrix Method (TMM) relates the inlet pressure (P_{in}) and inlet mass flow rate (V_{in}) to the outlet pressure (P_{out}) and the outlet mass flow rate (V_{out}) [8]. In this method, each element of the system is represented by a 2x2 matrix. Eq. (1) is the expression used to represent config. A, in which the first matrix on the right side of

the equation represents the secondary pipe, the second represents the plenum and the third represents the primary pipes (manifold runners).

$$\begin{bmatrix} P_{in} \\ \dot{V}_{in} \end{bmatrix} = \begin{bmatrix} cos(kL_1) & j\frac{\rho c}{A} sen(kL_1) \\ j\frac{A}{\rho c} sen(kL_1) & cos(kL_1) \end{bmatrix} \begin{bmatrix} co\,s(kL_{Pl}) & j\frac{\rho c}{A_{Pl}} sen(kL_{Pl}) \\ j\frac{A_{Pl}}{\rho c} sen(kL_{Pl}) & co\,s(kL_{Pl}) \end{bmatrix} \begin{bmatrix} 1 & 1 \\ n/Z_{OC} & 1 \end{bmatrix} \begin{bmatrix} P_{out} \\ \dot{V}_{out} \end{bmatrix} \quad (1)$$

Where k is the wave number define as the angular frequency ($2\pi f$) divided by the speed of sound in the air (c), A is the pipe's area, L_1 is the secondary pipe's length, L_{Pl} is the plenum's length, ρ is the air density and n is the number of primary pipes. The open-closed pipe impedance (Z_{OC}) is given by eq. (2).

$$Z_{OC} = -j\frac{\rho.c}{A} cot\left(\frac{2.\pi.f}{c}.L\right) \quad (2)$$

The multiplication of the firsts three matrices on the right side of eq. (1) results in the transfer matrix of config. A, where L_{pl} and A_{pl} are the plenum's length and the transversal area, Z_{OC} is the impedance of the closed-open pipe, which is given by eq. (2). The system's equivalent admittance is given by dividing the term of the first row and first column by the term of the second row and first column of the transfer matrix. The terms of the imaginary part (which are multiplied by j) have to be zero to be possible to find the natural frequency.

Similarly, the multiplication of the first three matrices on the right side of eq. (3) results in the transfer matrix of config. B, where Z_{RD} is given by eq. (4). The system's equivalent admittance is given by dividing the term of the first row and first column by the term of the second row and first column of the transfer matrix. The terms of the imaginary part (which are multiplied by j) have to be zero to be possible to find the natural frequency.

$$\begin{bmatrix} P_{in} \\ \dot{V}_{in} \end{bmatrix} = \begin{bmatrix} cos(kL_3) & j\frac{\rho c}{A} sen(kL_3) \\ j\frac{A}{\rho c} sen(kL_3) & cos(kL_3) \end{bmatrix} \begin{bmatrix} 1 & 1 \\ \frac{1}{Z_{RD}} & 1 \end{bmatrix} \begin{bmatrix} cos(kL_2) & j\frac{\rho c}{A} sen(kL_2) \\ j\frac{A}{\rho c} sen(kL_2) & cos(kL_2) \end{bmatrix} \begin{bmatrix} cos(kL_{Pl}) & j\frac{\rho c}{A_{Pl}} sen(kL_{Pl}) \\ j\frac{A_{Pl}}{\rho c} sen(kL_{Pl}) & cos(kL_{Pl}) \end{bmatrix} \begin{bmatrix} 1 & 1 \\ \frac{n}{Z_{OC}} & 1 \end{bmatrix} \begin{bmatrix} P_{out} \\ \dot{V}_{out} \end{bmatrix} \quad (3)$$

$$Z_{RD} = j\frac{\rho}{\omega A_{p1}} \frac{L_{p1}L_{p2}(2.\pi.f)^4 - c^2\left[L_{p1}A_{p2}\left(\frac{1}{V_{c1}}+\frac{1}{V_{c2}}\right) + L_{p2}A_{p1}\frac{1}{V_{c1}}\right](2.\pi.f)^2 + \frac{c^4 A_{p1}A_{p2}}{V_{c1}V_{c2}}}{c^2 A_{p2}\left(\frac{1}{V_{c1}}+\frac{1}{V_{c2}}\right) - L_{p2}(2.\pi.f)^2} \quad (4)$$

3 Methodology

In order to analyze the airflow through the intake manifold and the impact of the pulsating pressure wave phenomena in the flow rate, both experimental and numerical methodologies were applied in this work.

3.1 Experimental Setup

The flow test bench of the Applied Fluid Dynamics Laboratory at PUC Minas used to carry out the experiments is shown in Fig. 2. This test rig is capable of reproducing fluid flow conditions in a steady and unsteady regimes in the intake and exhaust manifolds. In the unsteady conditions, the flow test bench aims to reproduce the pulsating phenomena produced by the movement of the valves so that is possible to analyze the resonance effects which arise with the interaction of the air flow and the geometry of the intake (or exhaust) system installed in it.

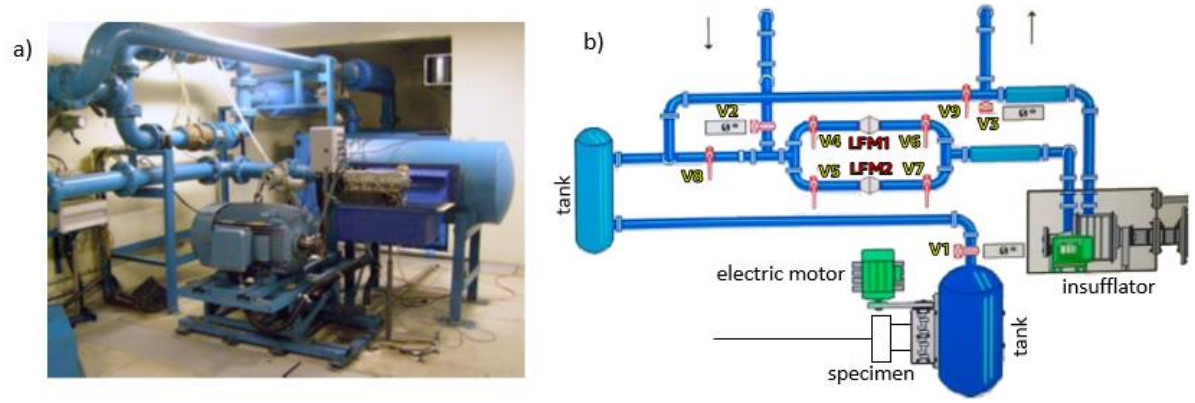

Figure 2. Flow test bench (a) and its diagram (b).

As it can be seen in scheme shown in Fig. 2 (b), the flow bank consists of an air insufflator, two pressure equalization tanks, pipelines, valves (V1 to V9), two laminar flow meters (LFM1 and LFM2), an electric motor and the sample which it is been tested (in this case the cylinder head and the intake manifold). The air insufflator generates a depression in the pipeline that connects it with the pressure equalization tank. These pipelines have valves that allow flow control and also allow flow direction depending on which set of valves is open. The laminar flow meters are used to determine the air mass flow rate. One of the pressure equalization tanks is connected directly to the cylinder head and its main function is to provide a constant pressure difference between the atmosphere and the tank itself, since the pistons have been removed from the engine and the pulsating phenomena are influenced only by the movements of the intake valves. Two sets of intake manifolds have been tested: the first is composed by the intake manifolds installed at the entrance of cylinders two and four, whereas the other cylinders had their inlets sealed and their valves removed. The second set comprising intake manifolds installed at the entrance of the four cylinders. The electric motor was coupled to the pulley of the camshaft by means of a set of pulley and timing belt. The engine induction order is 1-3-4-2.

3.2 Numerical Code

The simulations were performed using a computational code which applies the Characteristics Method to solve the Hyperbolic Partial Differential Equations (HPDE) of the studied flow. The initial and boundary conditions are taken from the experimental data collected, using rectangular meshes in time and space to solve the conservation of mass, momentum and ideal gas equations (Eqs. 5-7).

$$\frac{1}{\rho}\frac{\partial \rho}{\partial t} + \frac{u}{\rho}\frac{\partial \rho}{\partial x} + \frac{\partial u}{\partial x} = 0 \tag{5}$$

$$\frac{\partial u}{\partial t} + u\frac{\partial u}{\partial x} + \frac{1}{\rho}\frac{\partial p}{\partial x} = 0 \tag{6}$$

$$c^2 = \frac{\gamma \cdot p}{\rho} \tag{7}$$

Where γ is the ratio between the specific heats and u is the fluid speed. The technique for solving these equations using the Characteristic Method was previously detailed by Benson [17].

4 Results and Discussion

The air mass flow rate as a function of the camshaft speed for all four configurations is shown in Fig. 3. The average mass flow is 32.90 g/s for the numerical simulations and 33.14 g/s for the experimental tests for the config. A2, while the config. B2 has a 36.08 g/s (numerical) and 35.68 g/s (experimental) average air mass flow rate.

Regarding to the intake manifolds composed four cylinders, the config. A4 has a 68.23 g/s (numerical) and 68.13 g/s (experimental) average air mass flow rate, while the config. B4 has a 69.59 (numerical) and 69.24 g/s (experimental) average air mass flow rate. The experimental uncertainties are also shown. It is possible to observe a good agreement between the numerical and experimental curves. There is a minimum flow rate value for the config. A2 at the speed of 1200 rpm, the occurrence and location of this point will be discussed.

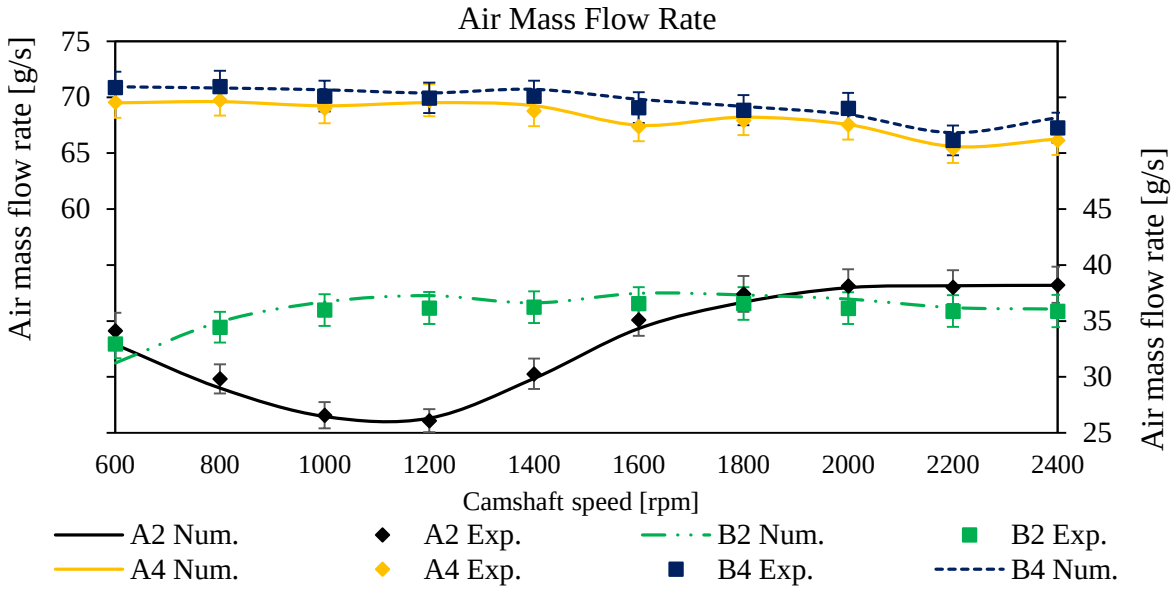

Figure 3. Air mass flow rate as a function of camshaft speed for all four configurations.

Unlike what happened in the air mass flow rate curve for the two-cylinders intake manifolds when comparing the configuration without double resonator (A2) to the one with the double resonator (B2), the four-cylinders intake manifolds did not have expressive increase in the flow rate. In fact, the air mass flow rate was increased in 38.6%, in the speed of 1200 rpm, when it was inserted the resonator in the two-cylinders intake manifold. On the other hand, the higher increase in the four-cylinders intake manifolds after the insertion of the resonator was only 3.4% in the speed of 1600 rpm. The Tab. 2 shows the results of application of the Transfer Matrix Method by means of the Eqs. (1) and (3) to calculate the natural frequency for all four configurations. Note that the natural frequency of configuration A2 occurs in the minimum point of the air mass flow rate curve. Besides, the natural frequency for each configurations is a little higher for four cylinders compared to two cylinder layouts.

Table 2. Natural frequency of all four configurations (inside parentheses: Hz, outside: rpm)

Frequency	A2	A4	B2	B4
1th	18.59 (1115)	16.31 (978)	28.55 (1713)	28.87 (1732)
2th	-	-	36.60 (2196)	40.04 (2400)

The transient air mass flow rate curves for the cylinder 4 are shown in the Fig. 4. The speed analyzed is 1200 rpm, which is the minimum flow rate value for the config. A2 shown in the Fig. 3. It can be observed that the conf. B2 has a higher area below the air mass flow rate curve compared to conf. A2. The larger is this area, the bigger is the mean flow rate value (Fig. 3). This increase in the mean flow rate value happens because of the insertion of the Helmholtz resonator, which decreases the pressure oscillation in the intake manifold.

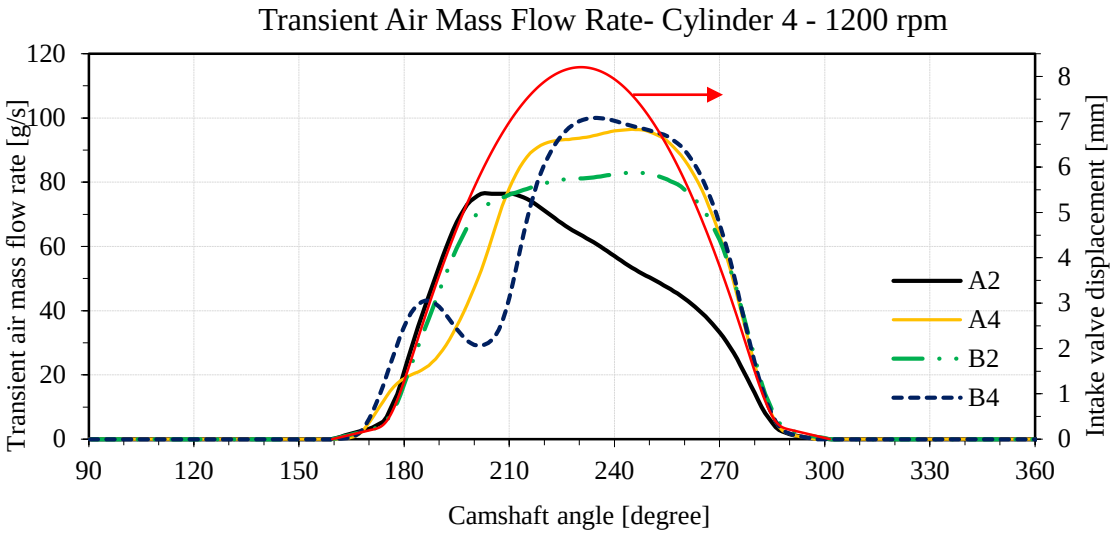

Figure 4. Air mass flow rate as a function of camshaft angle for cylinder 4 at 1200 rpm.

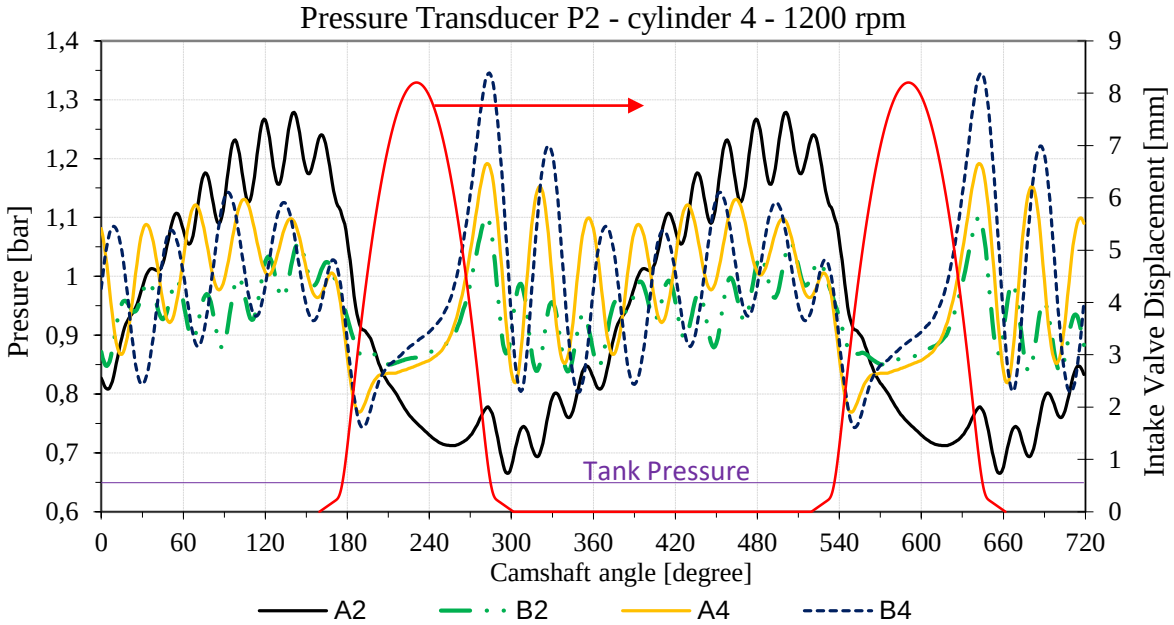

Figure 5. Air pressure as a function of camshaft angle for cylinder 4 at 1200 rpm.

The pressure curves in the intake valve port of the cylinder 4 at 1200 rpm are shown in Fig. 5. As expected, the config. A2 pressure in the intake valve port drops drastically to a value near the equalization tank pressure as soon as the intake valve starts to open at 159.5° of the camshaft. This is the main reason why there is a minimum point for the config. A2 at 1200 rpm in Fig. 3: the absence of the Helmholtz resonator, which allows the pressure waves to oscillate in a high level. Config. A4, on the other hand, does not have a similar behavior due to the reflection of the pressure wave inside the plenum can return to one of four cylinder, not one of two as it happens for two-cylinders configurations.

5 Conclusions

It is possible to observe a good agreement between the numerical and experimental curves, which indicates that the Characteristics Method is capable of reproducing the pulsating phenomena that occur in the admission system. The insertion of the double-chamber Helmholtz resonator increased the air mass flow rate more significantly in the four-cylinders compared to the two-cylinders configurations. The two-cylinders configurations had an increase in flow rate was of 38.6% in the speed of 1200 rpm, while the higher increase in the four-cylinders

with the insertion of the resonator was only 3.4% in the speed of 1600 rpm. The minimum point for the flow rate curve of the config. A2 at 1200 rpm is due to the absence of the Helmholtz resonator, which allows the pressure waves to oscillate in a high level. Four-cylinders configurations, on the other hand, does not have a similar behavior due to the reflection of the pressure wave inside the plenum can return to one of the four cylinder, not one of the two as it happens for two-cylinders configurations.

Acknowledgements. The authors thank the Brazilian National Council for Scientific and Technological Development (CNPq), the Coordination for the Improvement of Higher Education Personnel (CAPES), the Foundation of Support Research of the State of Minas Gerais (FAPEMIG) and the Pontifical Catholic University of Minas Gerais for the financial support of this project by means of the Research Incentive Fund (FIP - 2019/22451).

Authorship statement. The authors hereby confirm that they are the sole liable persons responsible for the authorship of this work, and that all material that has been herein included as part of the present paper is either the property (and authorship) of the authors, or has the permission of the owners to be included here.

References

[1] Benajes J, Reyes E, Galindo J, Peidro J. "Predesign Model for Intake Manifolds in Internal Combustion Engines". *SAE Tech Pap* 1997:14. https://doi.org/https://doi.org/10.4271/970055.
[2] Hanriot S de M, Queiroz JM, Maia CB. "Effects of variable - volume Helmholtz resonator on air mass flow rate of intake manifold". *J Brazilian Soc Mech Sci Eng* 2019;41:1–14. https://doi.org/10.1007/s40430-019-1566-5.
[3] Ohata A, Ishida Y. "Dynamic Inlet Pressure and Volumetric Efficiency of Four Cycle Four Cylinder Engine". *SAE Tech Pap Ser* 1982:14. https://doi.org/10.4271/820407.
[4] Winterbone DE, Pearson RJ. "Design techniques for engine manifolds: wave action methods for IC engines". *Professional Engineering Pub. Limited*; 1999.
[5] Hanriot SM. Estudo dos fenômenos pulsantes do escoamento de ar nos condutores de admissão em motores de combustão interna. Universidade Federal de Minas Gerais, 2001.
[6] Igarashi J, Masaaki A. "Fundamentals of acoustical silencers: Attenuation characteristics studied by an eletric simulator". *Aeronaut Res Insitute* - Univ Tokyo 1960:15.
[7] Igarashi J, Toyama M. "Fundamentals of acoustical silencers: Theory and experiment of acoustic low-pass filters". *Aeronaut Res Insitute* - Univ Tokyo 1958:19.
[8] Igarashi J, Miwa T. "Fundamentals of acoustical silencers: Determination of four terminal constants of acoustical elements". *Aeronaut Res Insitute* - Univ Tokyo 1959:67–85.
[9] Munjal ML. "Velocity ratio-cum-transfer matriz method for the evaluation of a muffler with mean flow". *J Sound Vib* 1975;39:105–19.
[10] Cai C, Mak CM. "Acoustic performance of different Helmholtz resonator array configurations". *Appl Acoust* 2018;130:204–9. https://doi.org/10.1016/j.apacoust.2017.09.026.
[11] CAI C, MAK CM. "Noise attenuation capacity of a Helmholtz resonator". *Adv Eng Softw* 2018;116:60–6. https://doi.org/10.1016/j.advengsoft.2017.12.003.
[12] Bortoluzzi D, Cossalter V, Doria A. "The Effect of Tunable Resonators on the Volumetric Efficiency of an Engine". *SAE Tech Pap Ser* 1998;2:12. https://doi.org/https://doi.org/10.4271/983045.
[13] Hanriot SM, de Medeiros MAF, Sodré JR, Valle RM. "An Experimental and Numerical Study from Pulsating Flow in Intake Manifold". *SAE Tech Pap Ser* 2000:10. https://doi.org/https://doi.org/10.4271/2000-01-3162.
[14] Queiroz JM. Influência de um Ressonador de Volume Variável na Vazão Mássica de um Motor de Combustão Interna. Pontifícia Universidade Católica de Minas Gerais, 2011.
[15] Queiroz JM. Influência de Ressonador de Helmholtz e da Geometria do Sistema de Admissão na Vazão de Ar de um Motor de Combustão Interna. Pontifícia Universidade Católica de Minas Gerais, 2015.
[16] Hanriot SM, Queiróz JM, Maia CB. "Influence of transient phenomena in the discharge coefficient through the intake valve in an internal combustion engine". *10th Int. Conf. Heat Transf. Fluid Mech. Thermodyn.*, Orlando, Florida: HEFAT 2014; 2014, p. 1632–8.
[17] Benson RS, Horlock JH, Winterbone DE. The thermodynamics and gas dynamics of internal combustion engines. Oxford: Clarendon Press; 1982.